

Directed random walks in continuous space

Sheng-You Huang, Xian-Wu Zou,* and Zhun-Zhi Jin

Department of Physics, Wuhan University, Wuhan 430072, People's Republic of China

(Received 6 January 2002; published 20 May 2002)

The investigation on diffusion with directed motion in a two-dimensional continuous space is completed by using the model of the continuous directed random walks. The average square end-to-end distance $\langle R^2(t) \rangle \sim t^{2\nu}$ is calculated. The results show that this type of walks belongs asymptotically to the same class ($\nu = 1.0$) as the ballistic motions. For short time, we observe a crossover from purely random walks ($\nu = 0.5$) to ballistic motions ($\nu = 1.0$). The dependence of the crossover on the direction parameter θ is studied. There exists a scaling relation of the form $\langle R^2(t) \rangle \sim t f(t/\theta^{-2})$. The return probability $P_{00}(t)$ is also investigated and the scaling form similar to $\langle R^2(t) \rangle$ is obtained.

DOI: 10.1103/PhysRevE.65.052105

PACS number(s): 05.40.Fb, 61.41.+e

In the past few decades, based on simple Brownian motion, various models of random walks (RW) with memory or interaction have been studied in order to account for distinct features of physical, chemical, and biological systems, whose complexity goes beyond what can be obtained from the simple random walk picture [1–8]. The standard RW, with isotropic diffusion, is a powerful tool for studying several physical processes such as diffusion, transportation [9], aggregation, structure formation [10,11], and diffusion controlled reactions [12].

Recently, the RW with anisotropy have extensively attracted a great deal of attention [13–15]. This type of anisotropic systems is very common in nature, such as the porous reservoir rocks [16], the epoxy-graphite disk composites [17], etc. The directed polymers have also been investigated [18,19] because of their versatile applications ranging from growing interface to spin glasses and to flux lines in high T_c superconductors [20]. The directed self-avoiding walk model in lattice space has been used for studying directed polymers [21,22]. Because the model introduces a global bias in geometrical models it leads to novel anisotropic critical behavior [14]. Asymptotically, it is found for the two-dimensional case that the displacements $\langle R_{\parallel N} \rangle \sim \langle R_N^2 \rangle^{1/2} \sim N$ and $\langle R_{\perp N}^2 \rangle^{1/2} \sim N^{1/2}$, where N is the number of steps in the walk, and \parallel and \perp refer to projections of the displacement parallel and perpendicular to the preferred axis of the walk, respectively [14]. The biased diffusion in anisotropic disordered systems has been investigated, which mimics a particle moving on an anisotropic amorphous material [23]. It shows a transition from pure to drift diffusion when the bias reaches a threshold.

Previous RW with anisotropy have been studied on regular or fractal discrete lattices [13–15,18,20–23]. The walker has only several discrete moving directions. In fact, the walking space is not discrete and is continuous. In this paper we present a continuous-space directed random walk (CDRW) model in order to extend these anisotropic motions in discrete space to continuous space. For the present model

the walker can perform any number of time steps or walk any distance of length. Therefore, no finite-size effects exist in the simulations.

In the CDRW model the walker moves on a continuous plane and has a preferential direction (+ x axis here). The moving direction of the walker can be determined as follows. The direction parameter is introduced via an angle θ . First we draw the extension against the preferential direction. This extension is considered to be the dichotomy of the new angle θ , i.e., an angle of $\theta/2$ is formed above the extension, and $\theta/2$ below it. Then, we make the supplementary angle γ ($= 2\pi - \theta$) of θ , and take a random direction in this γ angle as the moving direction of the walker for the next step. Such a schematic diagram is shown in Fig. 1, where $\gamma = 90^\circ$ and $\theta = 270^\circ$. It is obvious that as $\theta \neq 0$ the motion of the walker is anisotropic. The larger the θ is, the stronger is the anisotropy of motion.

Monte Carlo (MC) simulations have been used to study the movement of the walker. In the simulations the reduced units were used. The MC step is taken as the time unit, and the walker moves a unit length for each step. To investigate the effect of direction parameter on the motion of the walker, the average square end-to-end distance $\langle R^2(t) \rangle$ is calculated for a series of θ values in the interval $[0^\circ, 360^\circ]$. It is expected that this quantity scales with time t as

$$\langle R^2(t) \rangle \sim t^{2\nu}, \quad (1)$$

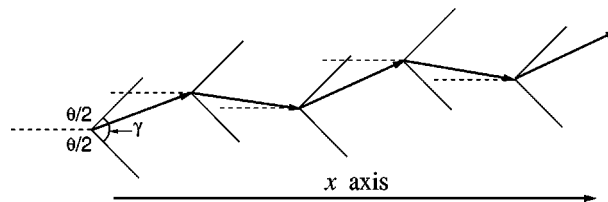


FIG. 1. A pictorial of directed motion in two-dimensional continuous space. The preferential direction is chosen as the x axis. Draw the extension against the preferential direction (dashed line) before each step. To regard the extension as the dichotomy form the angle θ . Then make its supplementary angle γ by the relationship $\gamma = 2\pi - \theta$. Take a random direction inside γ angle as the walking direction.

*Author to whom correspondence should be addressed. Email address: xwzou@whu.edu.cn

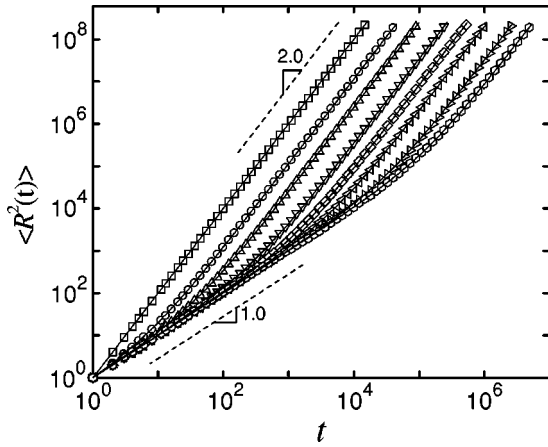


FIG. 2. The average square end-to-end distance $\langle R^2(t) \rangle$ as a function of time t for several θ values. From left to right $\theta = 360^\circ, 100^\circ, 50^\circ, 20^\circ, 10^\circ, 5^\circ, 2^\circ$, and 1° . The symbols are the simulation results and the lines are the plots of the analytic expression Eq. (8).

where $\langle \dots \rangle$ is the average over independent walk realizations. To reduce the effect of the fluctuation on calculated results, at least 1000 independent realizations were performed for each θ .

Figure 2 shows the $\langle R^2(t) \rangle$ as a function of t with θ ranging from 1° to 360° . It can be seen that when $\theta = 360^\circ$, the movement of the walker corresponds to the ballistic motion, and the $\langle R^2 \rangle$ - t relation can be described by a straight line with a slope of 2.0, as expected. It is also noted that when $\theta = 0$ the present motion reduces to purely RW with $2\nu = 1.0$. When $0^\circ < \theta < 360^\circ$, a crossover appears and there exists a crossover time t_c . As $t \ll t_c$, the slopes of curves are approximately equal to 1.0, and as $t \gg t_c$, the curves all bend toward the slope of 2.0. This asymptotic behavior is in agreement with the results for lattices [15,21,23]:

$$\langle R^2(t) \rangle = At^2 \quad t \rightarrow \infty. \quad (2)$$

It shows that as the time t approaches infinity, the average square end-to-end distance is proportional to t^2 with a proportional constant A . Therefore, the CDRW belongs to the same universality class as the simple ballistic motion. The direction factor A and the crossover time t_c are related to the direction angle θ . From Fig. 2 we can obtain the values of A and t_c for each θ . Figure 3 shows the plots of A and t_c as a function of θ .

Figures 2 and 3 can be explained as follows. We regard the CDRW as the motion in an invariant external field, which provides a preferential direction for the walker. Let the direction of the external field parallel to x axis. The field strength B , being $0 \leq B \leq 1$, can be given by the step probabilities in x direction as

$$B = p_{x+} - p_{x-}, \quad (3)$$

where p_{x+} and p_{x-} are the transition probabilities moving to positive and negative x directions, respectively. Thus, the displacement of the walker $\delta \vec{r}$ in a step can be expressed by

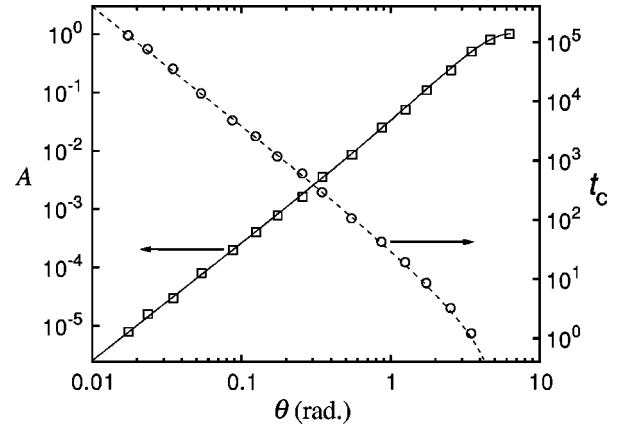


FIG. 3. The proportional constant A (\square) and crossover time t_c (\circ) as a function of the direction angle θ . The symbols are the simulation results. The solid and dashed lines are the plots of Eqs. (10) and (12), respectively.

$$\delta \vec{r} = \delta x \vec{e}_x + \delta y \vec{e}_y = \cos \phi + \sin \phi, \quad (4)$$

where ϕ is the angle between the moving direction of the walker and preferential direction. Therefore, the transition probabilities can be expressed in terms of ϕ as

$$p_{x+} = \langle \cos \phi \rangle |_{\cos \phi > 0} \quad (5a)$$

and

$$p_{x-} = -\langle \cos \phi \rangle |_{\cos \phi < 0}, \quad (5b)$$

$\langle \dots \rangle$ means the averaging over all possible moving directions, and the subscript expressions represent the limiting conditions. Combining Eqs. (3) and (5), the field strength B can be expressed as

$$B = \langle \cos \phi \rangle. \quad (6)$$

Calculating $\langle \cos \phi \rangle$ in the range of ϕ from $-(2\pi - \theta)/2$ to $(2\pi - \theta)/2$, we obtain $\langle \cos \phi \rangle = \sin(\theta/2)/(\pi - \theta/2)$. Combining this relation with Eq. (6) we get

$$B = \frac{\sin(\theta/2)}{\pi - \theta/2}. \quad (7)$$

It can be seen from Eq. (7) that as $\theta = 0$, the field strength $B = 0$ and the model reduces to purely RW; as $\theta = 360^\circ$, the field has the largest strength $B = 1$ and the model corresponds to the ballistic motion. By using stochastic methods, the analytic expression of $\langle R^2 \rangle$ as functions of t and B can be obtained as follows [24]:

$$\langle R^2(t) \rangle = (1 - B^2)t + B^2 t^2. \quad (8)$$

Combining Eqs. (7) and (8), we can calculate the time evolution of $\langle R^2 \rangle$ for given θ values. These calculated results are also shown in Fig. 2. As shown in the figure, the simulation results are very good in agreement with the theoretical values of Eq. (8).

When the time $t \rightarrow \infty$, Eq. (8) becomes

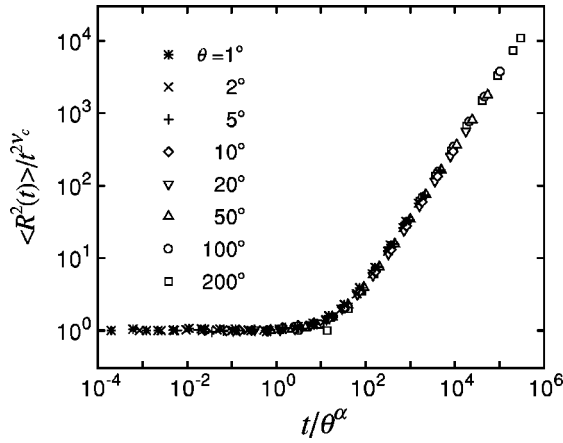


FIG. 4. Scaling plots of the average square end-to-end distance $\langle R^2(t) \rangle$. The data are quoted from Fig. 2. The scaling exponents $\nu_c = 1/2$ and $\alpha = -2$.

$$\langle R^2(t) \rangle = B^2 t^2. \quad (9)$$

It is just the case of ballistic motion. Combining Eqs. (2), (7), and (9), we obtain

$$A = \left(\frac{\sin(\theta/2)}{\pi - \theta/2} \right)^2. \quad (10)$$

The theoretical results of A from Eq. (10) are plotted in Fig. 3. It is evident that the simulation results of A are in good agreement with the prediction of Eq. (10).

According to Eq. (8), one can also find that as the field strength $B \ll 1$ (θ is very small), the coefficients $(1 - B^2) \gg B^2$. For short time the linear term $(1 - B^2)t$ controls the dynamics of CDRW comparing with the quadratic one $B^2 t^2$, and the curves have the slopes of $2\nu = 1.0$. While the time $t \rightarrow \infty$, the quadratic term $B^2 t^2$ is dominant, and the curves have the slopes of $2\nu = 2.0$ for all θ values, as expected (see Fig. 2). As these two terms are comparable to each other, the crossover occurs. Therefore, one can estimate the crossover time t_c by taking $(1 - B^2)t_c \approx B^2 t_c^2$, i.e.,

$$t_c = \frac{1 - B^2}{B^2}. \quad (11)$$

Substituting Eq. (7) into Eq. (11), the cross-over time t_c can be expressed in terms of θ as

$$t_c = \frac{(\pi - \theta/2)^2 - \sin^2(\theta/2)}{\sin^2(\theta/2)}. \quad (12)$$

The calculated t_c - θ relation is drawn in Fig. 3. This figure shows that the simulation result of t_c is in excellent agreement with the analytic values of Eq. (12) in the whole range of θ .

Going a step further, to understand the crossover behavior of $\langle R^2(t) \rangle$ we suggest the following scaling approach. As seen from above, the scaling behaviors of CDRW show a phase transition at the critical point $\theta_c = 0$. As $\theta = \theta_c$ the CDRW belongs to the purely RW class, and as $\theta > \theta_c$ the

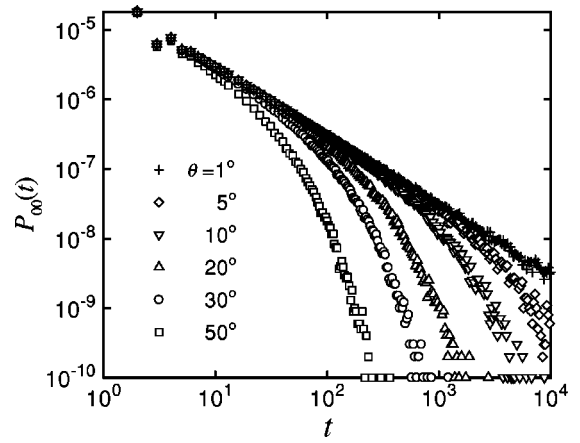


FIG. 5. The return probability $P_{00}(t)$ as a function of time t for a set of θ values. These data are averages of 10^6 realizations.

CDRW falls into the same universality class as the ballistic motion. Guided by Fig. 2, it is expected that there exists the scaling relation of the form

$$\langle R^2(t) \rangle \sim t^{2\nu_c} f(t/t_c), \quad (13a)$$

where

$$t_c \sim (\theta - \theta_c)^\alpha, \quad (13b)$$

and ν_c is the so-called critical exponent with $\langle R^2(t) \rangle \sim t^{2\nu_c}$ for $\theta = \theta_c$ [8]. It is easy to obtain the critical exponent $\nu_c = 0.5$. The exponent α has to be determined numerically. As t_c is the only relevant time scale, the scaling functions bridge the short time and the long time regime. To match both regimes, the scaling function $f(x)$ has the form of $f(x) = \text{const}$ for $x \ll 1$, and $f(x) \sim x^{2-2\nu_c}$ for $x \gg 1$.

To test the scaling relation (13) and to determine the exponent α , we plotted $\langle R^2(t) \rangle / t^{2\nu_c}$ as a function of t/t_c for a set of θ values. At $\alpha \approx -2$ the best data collapse is obtained and is shown in Fig. 4. The excellent data collapse strongly supports the above scaling assumptions.

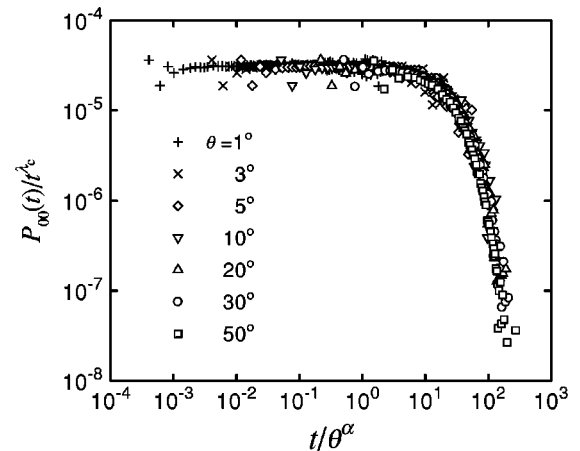


FIG. 6. Scaling plots of the return probability $P_{00}(t)$ for a set of θ values. The data are taken from Fig. 5. The scaling exponents $\lambda_c = -1$ and $\alpha = -2$.

We also investigated the scaling behavior of the return probability $P_{00}(t)$, which is the probability of the walker returning to the original site. For the CDRW the walker cannot return to the origin (0,0) exactly, so we make a rule that if the walker enters the area limited by $(\pm 0.5, \pm 0.5)$, this walker is regarded as that returning to the original site. To get accurate average value of $P_{00}(t)$ we have used 10^6 realizations for each θ . For each simulation, 10^4 time steps are taken.

Figure 5 plots the results of $P_{00}(t)$ for several θ values. It can be seen that for a small value of θ the behavior of $P_{00}(t)$ bears analogy with the case of purely RW, i.e., $P_{00}(t) \sim t^{\lambda_c}$ with $\lambda_c = -1$, and for large θ , $P_{00}(t)$ decays exponentially. Similar to Eq. (13), a scaling expression is valid for the return probability $P_{00}(t)$

$$P_{00}(t) \sim t^{\lambda_c} g(x), \quad (14)$$

where $g(x)$ is a rapidly decaying scaling function with the

limit $g(x) = \text{const}$ for $x \ll 1$. However, the argument of $g(x)$ should have the same form as that of $f(x)$ in Eq. (13), namely $x = t/\theta^\alpha$. Figure 6 shows the scaling plots of $P_{00}(t)$ for several θ values. It will be seen from this that the scaling expression (14) is suitable for $P_{00}(t)$.

In summary, we present a method to investigate the directed random walks in continuous space. Using the method the average square end-to-end distance $\langle R^2(t) \rangle \sim t^{2\nu}$ is calculated. The scaling behavior of present motions belongs asymptotically to that of ballistic motions. For short time, a crossover from purely RW ($\nu = 0.5$) to ballistic motions ($\nu = 1.0$) is observed. The scaling relation of the form $\langle R^2(t) \rangle \sim t f(t/\theta^{-2})$ is obtained. Analogous scaling relation is also found for the return probability $P_{00}(t)$.

This work was supported by the National Natural Science Foundation of China.

-
- [1] B.D. Hughes, *Random Walks and Random Environments* (Clarendon Press, Oxford, 1995); G. H. Weiss, *Aspects and Applications of the Random Walk* (North-Holland, Amsterdam, 1994).
- [2] P. G. de Gennes, *Scaling Concepts of Polymer Physics* (Cornell University, Ithaca, 1979).
- [3] H.E. Stanley, K. Kang, S. Redner, and R.L. Blumberg, Phys. Rev. Lett. **51**, 1223 (1983); **54**, 1209 (1985); S. Redner and K. Kang, *ibid.* **51**, 1729 (1983).
- [4] H.C. Oettinger, J. Phys. A **18**, L363 (1985); P.M. Duxbury and S.L.A. de Queiroz, *ibid.* **18**, 661 (1985).
- [5] S.-Y. Huang, X.-W. Zou, W.-B. Zhang, and Z.-Z. Jin, Phys. Rev. Lett. **88**, 056102 (2002).
- [6] Z.-J. Tan, X.-W. Zou, S.-Y. Huang, W. Zhang, and Z.-Z. Jin, Phys. Rev. E **65**, 041101 (2002); Z.-J. Tan, X.-W. Zou, W. Zhang, and Z.-Z. Jin, Phys. Lett. A **289**, 251 (2001).
- [7] C. Domb, J. Stat. Phys. **30**, 425 (1983); D.J. Amit, G. Parisi, and L. Peliti, Phys. Rev. B **27**, 1635 (1983); V.B. Sapozhnikov, J. Phys. A **27**, L151 (1994).
- [8] A. Ordemann, E. Tomer, G. Berkolaiko, S. Havlin, and A. Bunde, Phys. Rev. E **64**, 046117 (2001).
- [9] *Fractals and Disordered Systems*, edited by A. Bunde and S. Havlin (Springer-Verlag, Berlin, 1991).
- [10] T. Vicsek, *Fractal Growth Phenomena* (World Scientific, Singapore, 1992).
- [11] A.-L. Barabási and H.E. Stanley, *Fractal Concepts in Surface Growth* (Cambridge University Press, Cambridge, 1995).
- [12] *Nonequilibrium Statistical in One Dimension*, edited by V. Privman (Cambridge University Press, Cambridge, 1997).
- [13] E.R. Reyes, M.O. Cáceres, and P.A. Pury, Phys. Rev. B **61**, 308 (2000).
- [14] S. Redner and I. Majid, J. Phys. A **16**, L307 (1983); J.J. Rajasekaran and S.M. Bhattacharjee, *ibid.* **24**, L371 (1991); S. Elezović-Hadžić and N. Vasiljević, *ibid.* **32**, 1329 (1999).
- [15] Lj. Budinski-Petković and U. Kozmidis-Luburić, Physica A **262**, 388 (1999); O. Bénichou, A.M. Cazabat, M. Moreau, and G. Oshanin, *ibid.* **272**, 56 (1999).
- [16] J.M.V.A. Koelman and A. de Kuijper, Physica A **247**, 10 (1997).
- [17] A. Celzard, G. Furdin, J.F. Marêché, E. Mcrae, M. Dufort, and C. Deleuze, Solid State Commun. **92**, 377 (1994).
- [18] M. Kardar and Y.C. Zhang, Phys. Rev. Lett. **58**, 2087 (1987); Y.C. Zhang, *ibid.* **59** (1987).
- [19] E. Perlsman and S. Havlin, Phys. Rev. E **63**, 010102(R) (2001).
- [20] S.B. Santra, W.A. Seitz, and D.J. Klein, Phys. Rev. E **63**, 067101 (2001).
- [21] V. Privman and N.M. Svrakic, *Directed Models of Polymers, Interface, and Clustering: Scaling and Finite Size Properties*, Lecture Notes in Physics Vol. 38 (Springer, Berlin, 1989).
- [22] M.E. Fisher and M.E. Sykes, Phys. Rev. **114**, 45 (1959).
- [23] S. Bustingorry, E.R. Reyes, and M.O. Cáceres, Phys. Rev. E **62**, 7664 (2000).
- [24] J.W. Haus and K.W. Kehr, Phys. Rep. **150**, 263 (1987); J.P. Bouchaud and A. Georges, *ibid.* **195**, 127 (1990).